A Diode-Aware Model of PV Modules from Datasheet Specifications

Sara Vinco, Yukai Chen, Enrico Macii and Massimo Poncino
Politecnico di Torino, Turin, Italy
{name.surname}@polito.it

***Abstract*—Semi-empirical models of photovoltaic (PV) modules based only on datasheet information are popular in electrical energy systems (EES) simulation because they can be built without measurements and allow quick exploration of alternative devices. One key limitation of these models, however, is the fact that they cannot model the presence of bypass diodes, which are inserted across a set of series-connected cells in a PV module to mitigate the impact of partial shading; datasheet information refer in fact to the operations of the module under uniform irradiance. Neglecting the effect of bypass diodes may incur in significant underestimation of the extracted power.**

This paper proposes a semi-empirical model for a PV module, that, by taking into account the only available information about bypass diodes in a datasheet, i.e., its number, by a first downscaling the model to a single PV cell and a subsequent upscaling to the level of a substring and of a module, allows to take into accout the diode effect as much accurately as allowed by the datasheet information.

Experimental results show that, in a typical PV array on a roof, using a diode-agnostic model can signifantly underestimate the output power production.

I. Introduction

The landscape of simulation models for PV cells/modules is extremely vast, and the literature provides PV models with a large spectrum of accuracy/complexity tradeoffs [1]. One critical issue of all models is that the process of identifying its parameters is generally difficult, and would in principle require measurements.

Some models avoid this problem by using only information that can be obtained from the datasheet of PV modules. Fitting "public" information to a model template is easily manageable for semi-empirical models, where generic equations are used to fit the I-V curves provided in most datasheets (e.g, [2]), which are however less popular. Most models in fact rely on a classical single- or double-diode electrical circuit equivalent of a PV module; in this case the identification of the model parameters is more articulated and requires sophisticated algorithms to solve recurrent equations, and, more importantly, to make assumptions about the technology [3]–[10].

There is however one problem that current datasheet-based models do not consider: the information in the datasheet refers to a PV module (i.e. the "commercial" PV element) that consists, in modern devices, of the series connection of PV cells. I-V curves in a datasheet, which are the key information used to derive the models, are measured at the manufacturers' side *assuming that all cells of the PV module work at the same environmental conditions (irradiance and temperature)*.

This is clearly not always the case in a realistic installation, where *partial shadings* of a module can occur. In principle, in a series connection of PV cells, one fully shaded cell suffices to "clog" the current flow and to completely nullify the power generation of an entire module. To avoid this situation, cells in a module are grouped in shorter substrings and protected by a *bypass diode*, whose purpose is to reduce the worst case of a zero power generation by bypassing the substring containing a shaded cell. For instance, using 3 diodes in a PV module with 72 cells, the case of one shaded cell will result into the generation of 2/3 of the expected power: only the shaded substring will be bypassed.

It is evident that, if the model relies only on datasheet information that refers to the whole PV module, the effect of diodes cannot be taken into account. *All models based on datasheet are thus diode-agnostic*, and will underestimate power generation in conditions of partial shading.

To the best of our knowledge, this work is the first one that deals with the above problem; while still using a PV module datasheet as a starting point, our model is *diode-aware*, and includes the number of diodes as a parameter of the model of a PV module. The key element in our modeling flow is the *down-scaling of the PV module data to the scale of a single PV cell*, and the eventual *up-scaling of the cell model to the scale of a diode-protected substring of PV cells*. This up/down scaling of I-V curves is not straightforward and includes some empirical fitting of the model parameters.

Simulation results exemplify the adoption of the proposed model in two scenarios: during the design of a PV on a heavily shaded roof, and to estimate power production of a well-designed PV installation against real data. Results will prove the impact of modeling the presence of diodes under heterogeneous shading conditions, plus the effectiveness of the proposed model, despite of being generated solely from information available in datasheets.

The paper is organized as follows. Section II outlines the necessary background. Section III presents the proposed PV model, whose adoption is exemplified in Section IV. Finally, Section V draws our concluding remarks.

II. Background

A. PV Cells, Modules, and Arrays

A photovoltaic (PV) cell is a semiconductor diode whose $p-n$ junction is exposed to light [11]: the incidence of light on the cell generates charge carriers that originate electric current. A PV cell is usually represented in terms of its electric equivalent, as shown in Figure 1: an equivalent current source I_{PV} induced by the light, shunted with a diode and resistor R_p and cascaded with a series resistor R_s [12].

978-3-9819263-4-7/DATE20/©2020 EDAA

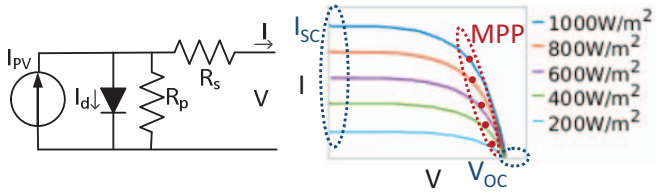

Figure 1. Circuit model of a PV cell (a), and characteristic I-V curve (b).

As any diode, the PV cell can be described analytically by means of a conventional diode equation, where the photocurrent I_{PV} has the effect of shifting the basic diode curve. Its I-V characteristics can be therefore expressed as:

$$I = I_{PV} - I_0\left[exp\left(\frac{qV}{akT}\right) - 1\right] \quad (1)$$

where V and I represent the output voltage and current of the solar cell, respectively, I_0 is the reverse saturation current of the diode, q is the electron charge, and a is a dimensionless constant that depends on technology. The resulting I-V curves (right of Figure 1) are characterized by their short circuit current I_{SC}, open-circuit voltage V_{OC}, and maximum power point (MPP), i.e., the maximum extracted power. Notice that the output current is strongly sensitive to solar irradiance.

A typical PV cell generates currents of a few amps and a voltage of about 0.6V. For this reason, cells are interconnected in series to form a *PV module*, and then PV modules are once again connected in series or in parallel into a *PV array*, to achieve the desired voltage and current levels.

B. Modeling PV Elements

The circuit of Figure 1 and Equation 1 are in principle suitable as a model for the whole hierarchy of PV elements: starting from a single cell, the series/parallel composition of a set of cells would be supported by simply connecting the cell models. The main limitation of such a circuit-equivalent model is the identification of the parameters [9], [10], [12]. Manufacturers never provide the values of the circuit elements; they rather disclose a number of I-V curves, and derating factors describing the dependence of power generation on irradiance and temperature. While it possible to identify the circuit parameters just from the information on a typical datasheet (e.g., [3], [4]), these methods require sophisticated algorithms to solve recurrent equations, and, more importantly, make assumptions about the technology of the underlying device (e.g., constant a). Therefore, a safe identification of these parameters would require measurements, which makes these models impractical. Moreover, there is another limitation related to the actual state of the art, as described in the next section.

C. Partial Shading and Diodes

Consider the case of two PV cells with different irradiance conditions connected in series (Figure 2); this is a quite typical situation that can occur due to a partial shading. This imbalance creates a potential electrical problem. As shown on the right of Figure 1, different irradiance translates into different currents; however, the two cells are forced to carry the same current as they are in series [13], [14]. To avoid potential heating problems, especially when the mismatch is significant, bypass diodes are used, as conceptually shown in Figure 2. If the input current does not exceed the current generation of the shaded cell, the two curves are combined as in ①, and both cells contribute to voltage. Otherwise, the shaded cell is bypassed through the diode; in this way the input current can flow, at the cost of some loss in the output voltage (②).

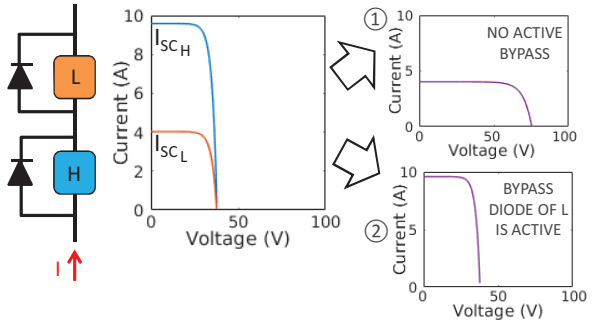

Figure 2. Bypass diodes (left), and impact of bypass diodes on the sum of I-V curves to reduce the impact of shading (right).

Figure 2 is however only conceptual: the larger the number of diodes the better, and ideally each cell in a module could have a bypass diode and the effect of a partial shading would be solved. However, the realistic configuration is to have *a set of series-connected PV cells that share a single diode*, for obvious cost reasons: the PV module market has very small margins and competition is fierce. A typical PV module in fact has 60 or 72 cells connected in series, and a number of blocking diodes (typically 3, in some cases 4); therefore, there is an intermediate level of hierarchy between cells and modules, which we call *the substring* (Figure 3).

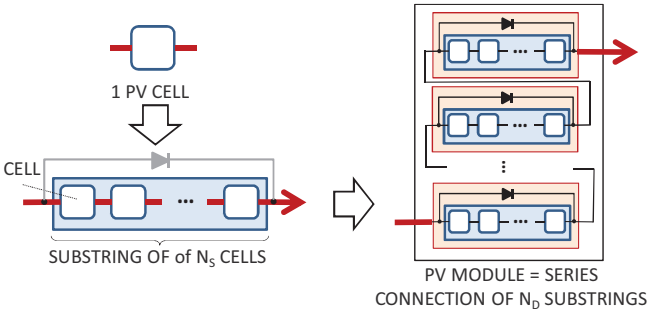

Figure 3. The PV hierarchy: cell, diode-protected substring, and module.

Although datasheets do usually report the number of PV cells and the number of diodes, the I-V curves do not reflect in any way the presence of diodes: they are derived *assuming that all cells of the PV module work at the same irradiance level*; therefore, existing modeling approaches that rely only on datasheet information cannot be "diode-aware". Neglecting the presence of diodes will underestimate power generation in conditions of partial shading.

III. Modeling Strategy

Figure 5 summarizes our modeling strategy; the minimum required information from the datasheet includes (i) I-V curves for a few irradiance levels, (ii) the number of PV cells N_C per module, (iii) the number of bypass diodes N_D, and (iv) the temperature derating coefficients of V_{OC} and I_{SC}. The latter information are not strictly necessary - in that case the model

will not be sensitive to temperature. An example of typical information is outlined in Figure 4, that shows the datasheet of the Peimar SG280P PV module [15], used in the experimental section.

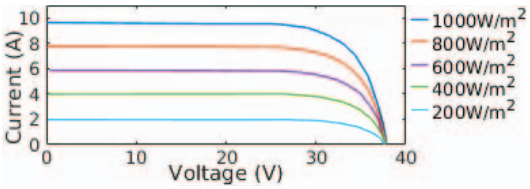

Rated Power (W)	280
# of PV cells (N_C)	60
# of diodes (N_D)	3
Temperature Coeff. on V_{OC}	-0.32%/°C
Temperature Coeff. on I_{SC}	-0.047%/°C

Figure 4. Datasheet information for the Peimar SG280P PV module [15].

Based on these information, the construction of the model goes through three main phases (Figure 5). In the first one (Section III-A), the module-level data in the datasheets are down-scaled to build the *current-voltage equation of a single cell*, as a function of irradiance G and temperature T. Then (Section III-B), by using the value N_D, the cell model is composed to get a *substring model*, i.e., a set of series-connected cell group under a single bypass diode. It is in this phase that the characteristics of the bypass diodes are taken into account, and the model of the PV module becomes diode-aware.
The substring model is then aggregated to obtain a *model of a PV module*; the latter is fact nothing but the interconnection of N_D substrings (Section III-C).
In a typical scenario, there is actually a fourth step, in which various PV modules are then interconnected into a PV array by means of given series/parallel topology (Section III-D). This step is completely identical to the case of a non diode-aware model of a module, so it will be discussed only with the purpose of introducing the simulation results.

A. Model of a Single PV Cell

1) I-V curves of a single PV cell: The I-V curves reported by datasheets usually refer to the entire PV module, and are extrapolated by assuming that diodes are not active, and that all PV cells are subject to the same irradiance and temperature. As a first step in this phase, the I-V curves are down-scaled so to derive the behavior of a single PV cell. This down-scaling strictly depends on the kind of interconnection between cells. In the typical case, all PV cells are connected in series: thus, this is achieved by simply dividing voltage (i.e., the x-axis) by the number of PV cells N_C. The scale on the current axis, conversely, does not change.
2) Estimation of V_{OC} and I_{SC}: From this point, the process follows the method described in [2], starting from the cell-level model. The second step is to derive expression for V_{OC} and I_{SC} for an individual cell as a function of G and T.
The dependence on G can be extrapolated from the cell-level I-V curves, i.e., the intercept of the curves on the two axis, that are used to empirically fit an equation of $I_{SC,cell}(G)$ and $V_{OC,cell}(G)$.

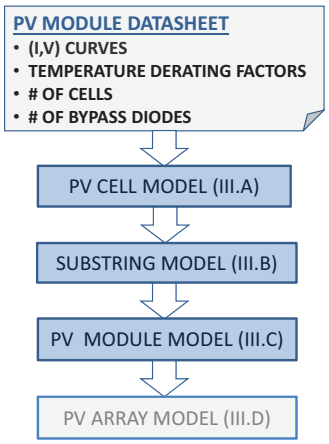

Figure 5. Overview of the Proposed Modeling Strategy.

Temperature dependence is instead typically exposed in datasheets as sensitivity coefficients ($\partial V_{OC}/\partial T$ and $\partial I_{SC}/\partial T$), that are used to correct the expressions of $I_{SC,cell}(G)$ and $V_{OC,cell}(G)$. The resulting equations are:

$$I_{SC,cell}(G,T) = I_{SC,cell}(G) \cdot \frac{\partial I_{SC}}{\partial T} \cdot \Big(T_{cell}(G,T) - T_{ref}\Big) \quad (2)$$

$$V_{OC,cell}(G,T) = V_{OC,cell}(G) \cdot \frac{\partial V_{OC}}{\partial T} \cdot \Big(T_{cell}(G,T) - T_{ref}\Big) \quad (3)$$

Notice that, in order to correctly model this dependency, cell temperature T_{cell} is first derived from ambient temperature T by using the relations in [16], which correlate it with G (as higher G results in higher T) and with other characteristic coefficients of the PV module[1].
3) I-V Curve Model of a PV cell: The third step consists of the empirical derivation of the I-V curves using Equations 2 and 3 as reference points.
Since the PV cell is a diode, we use the generic equation of the I-V characteristic of an *ideal* diode as a template to be fitted empirically, i.e., $I = I_{SC} \cdot a(e^{bV} - 1)$, where a and b lump the various electrical parameters of the diode.
In this generic equation, a represents a measure of the curvature of the I-V curve (larger values of a will "flatten" the curve). From the datasheet plot in Figure 4, we can see that the curvature of the I-V curves is quite dependent on irradiance; therefore, for accurate fitting, we cannot use a constant for a, which rather has to be made dependent on G. This is one distinctive point from the method of [2], where the fitting on the diode equation was done using a constant a as the equation referred to an entire module. In our case, since the cell-level equation will be re-scaled up to the level of a substring of several series-connected cells, the error would add up resulting in a significant error.
The diode equation is therefore transformed into:

$$I_{cell}(G,T) = I_{SC,cell}(G,T) - a(G) \cdot (e^{b \cdot V_{cell}} - 1) \quad (4)$$

where b is obtained by imposing that $I(V_{OC,cell}) = 0$:

$$b = V_{OC,cell}(G,T)^{-1} \cdot ln\big(1 + I_{SC,cell}(G,T) \cdot a(G)^{-1}\big) \quad (5)$$

[1] T_{ref} is the nominal temperature of the PV module.

Parameter a is derived as a function of G as follows: for each I-V cell-level curve, we first derive the corresponding value of a by fitting the curve to Equation 4; the values of a for each curve are then fitted to a polynomial $a(G)$[2].

B. Model of a Substring of Cells

A bypass diode is added around a substring of $N_S = N_C/N_D$ cells, where N_S is guaranteed to be an integer value as all substrings are made of the same number of PV cells.
To build the model of a substring, we first model the series connection of N_S cells using the cell-level model, and we eventually model the effect of the bypass diode.
In the series of N_S cells, the least irradiated cell constraints the current that can be generated by the overall series, whereas voltage is simply the sum of voltages of all cells (according to their irradiance). The resulting equation is:

$$\begin{array}{l} I_{SC,srs}(G,T) = min_i\big(I_{SC,cell,i}(G_i,T)\big) \\ V_{OC,srs}(G,T) = \sum_i V_{OC,cell(G_i,T),i} \\ I_{srs}(G,T) = I_{SC,srs}(min_i(G_i),T) - a(min_i(G_i)) \\ \qquad\qquad \cdot(e^{b\cdot V} - 1) \end{array} \tag{6}$$

where $i = 1, \ldots, N_s$ denotes the cells of the substring. The equation is exemplified in Figure 6 for three series-connected cells with different irradiance.

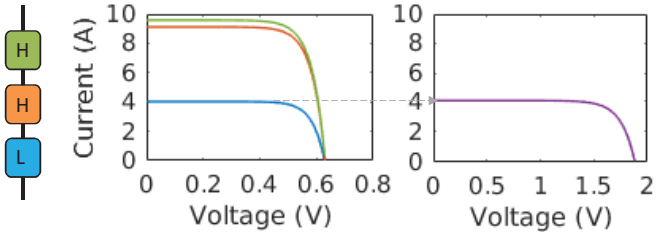

Figure 6. Architecture of three series connected cells controlled by a diode (left), corresponding I-V curves (middle), and I-V curve of their series connection (right, Equation 6).

The addition of the bypass diode determines the behavior of the substring when connected to other substrings. Assume that we are requested to pass a current I_{sub} through the substring. If this current is smaller than the current allowed by the most shaded cell (i.e., $I_{sub} \leq I_{SC,srs}$), then it will flow normally through the string of cells and the bypass diode is not activated. The voltage in this case can be calculated through the inverse function of Equation 4 scaled to one string, considering I as the free variable.
Otherwise (i.e., $I_{sub} > I_{SC,srs}$), the bypass diode is activated and the current finds a low-resistance path through the diode. The equivalent model of the substring is in this case a negative voltage drop $-V_F$, corresponding to the voltage drop across a forward-biased diode (specific of the type of diode, e.g., 0.6V for p-n junction diodes, 0.15V-0.45V for Schottky diodes).
The overall model of the substring is therefore:

$$V_{sub}(G,T) = \begin{cases} \ln\left(\frac{I_{sub}(G,T) - I_{SC,srs(G,T)}}{a} + 1\right) \cdot b^{-1}, \\ \qquad I_{sub} \leq I_{SC,srs} \\ -V_F, \qquad I_{sub} > I_{SC,srs} \end{cases} \tag{7}$$

[2]Note that we neglect the dependence of a on T since its impact on the internal resistance, and thus on the curvature, is negligible [13].

It is worth emphasizing that the addition of diode-awareness is the key novelty of our modeling framework. Other semi-empirical models such as [2] assume the presence of one diode across each smallest modeled object (i.e., a PV module). In our case, conversely, the smallest unit is a PV cell, and one diode "covers" multiple modeled objects.

C. Model of a PV module

Scaling up to the level of a PV module is straightforward. A PV module is the series connection of N_D substrings. Substring are independent of each other, but the combination of the models depends on the shading level of each substring, as shown in Equation 7.
Assuming a requested current I_{module} at the input of the series of substrings, PV module voltage is obtained by summing the voltage contribution of each substring:

$$V_{module}(G,T) = \sum_{j=1}^{N_D} V_{sub,j}(G_j,T) \tag{8}$$

This generates the classical I-V curve with multiple "steps", exemplified in Figure 7 for the connection of three substrings with bypass diodes. The operating point on the multiple "steps" curve is typically determined by a Maximum Power Point (MPP) tracking algorithm, and it is extracted as the maximum of the corresponding P-V curve.

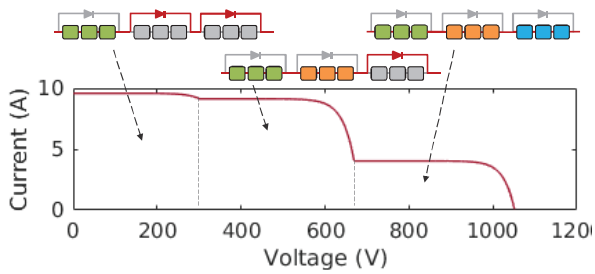

Figure 7. Example of multiple "steps" I-V curve generated by the connection of three substrings (with 3 bypass diodes).

D. Model of a PV array

PV modules are usually further interconnected together to form a PV array, and their connection in series or in parallel depends on the desired voltage and current levels. This step is therefore strongly dependent on the application context and is not strictly part of the methodology. To additionally combine the PV modules in series or in parallel, it is indeed possible to adopt state-of-the-art formulas [2], [13].
Given a $m \times n$ series-parallel interconnection of PV modules (i.e., n parallel strings each of m PV modules in series), the total power is obtained as $P_{array} = V_{array} \cdot I_{array}$, where:

$$\begin{cases} V_{array} &= \min_{j=1,\ldots,n}\left(\sum_{i=1,\ldots,m} V_{module,ij}\right) \\ I_{array} &= \sum_{j=1,\ldots,n}\left(\min_{i=1,\ldots,m} I_{module,ij}\right) \end{cases}$$

and $V_{module,ij}$ and $I_{module,ij}$ are the voltage and current extracted from the i-th module in the j-th string.

IV. Experimental Results

This section demonstrates the effectiveness of the proposed model. All simulations have been run in Matlab R2019a.

A. Design of a rooftop PV installation

As first experiment, we apply the proposed PV model in the context of the design of a PV installation on top of the roof of one industrial building.

1) Simulation Setup: The roof of interest is a lean-on roof oriented towards S-W with inclination 27°; its area suitable for PV installation is ≈5.4m×15.8m (represented by the black area on the left-hand side of Figure 8). The roof is subject to quite heterogeneous irradiance, caused by the neighbouring buildings projecting their shadows on different portions of the roof at different times of the day. This is evident from the heatmap of the average irradiance reported on the right-hand side of 8, where clearer areas are the most irradiated.

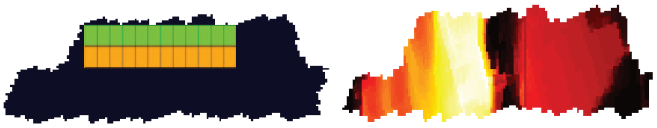

Figure 8. Placement of PV modules on the roof (left) and average distribution of irradiance on the roof (white $\approx 600W/m^2$, black $\approx 0W/m^2$, right).

The target installation is made of 24 PV modules, made of 2 series strings of 12 PV modules each. The adopted PV module is a PEIMAR SG280P PV module [15], with rated power 280W, 60 cells and 3 diodes. PV modules are placed on the roof with a compact placement, i.e., all PV modules are packed (left-hand side of Figure 8: rectangles of the same colors are PV modules connected in series). From Figure 8, it is evident that the PV modules are subject to quite heterogeneous irradiance: this will highlight the impact of shading on the behavior of the PV installation.

2) Application of the proposed PV model: Figure 9 exemplifies the adoption of the proposed model to the PEIMAR SG280P PV module. The Figure reports the equations modeling one cell of the PV module; the other equations are omitted as they do not contain PV module-specific coefficients. The Figure exemplifies also the process to derive $a(G)$, by showing the samples of a derived for the different values of G and the corresponding fitting polynomial.

$$V_{OC,cell}(G,T) = (1 - 3.2\text{e}{-3} \cdot (T_{cell}(G,T) - T_{ref})) \cdot \left(5.4\text{e}{-11} \cdot G^3 - 9.5\text{e}{-8} \cdot G^2 + 5.1\text{e}{-5} \cdot G + 0.6\right)$$

$$I_{SC,cell}(G,T) = (1 + 4.7\text{e}{-5} \cdot (T_{cell}(G,T) - T_{ref})) \cdot \left(1.8\text{e}{-9} \cdot G^3 - 3.7\text{e}{-6} \cdot G^2 + 0.01 \cdot G - 0.25\right)$$

$$a(G) = 1.12\text{e}{-16} \cdot G^4 - 2.85\text{e}{-13} \cdot G^3 + 2.35\text{e}{-10} \cdot G^2 - 7.75\text{e}{-8} \cdot G + 7.41\text{e}{-6}$$

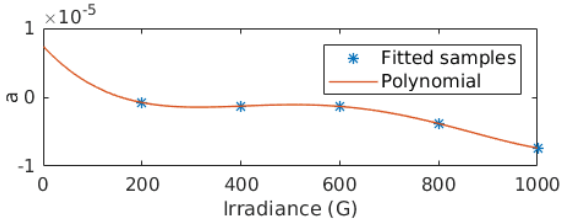

Figure 9. Equations for the cell model of a PEIMAR SG280P PV module (top), with estimated values of a and fitting polynomial (bottom).

3) Environmental traces: Environmental traces have been generated by adopting a GIS-based infrastructure like the one in [17], [18], that combines weather information and shadows models to generate irradiance and temperature traces with a 15-minute temporal resolution. The roof is aligned with a virtual grid, whose elements have size equal to the size of one PV cell, so that one value of temperature and irradiance is available for each PV cell at any time.

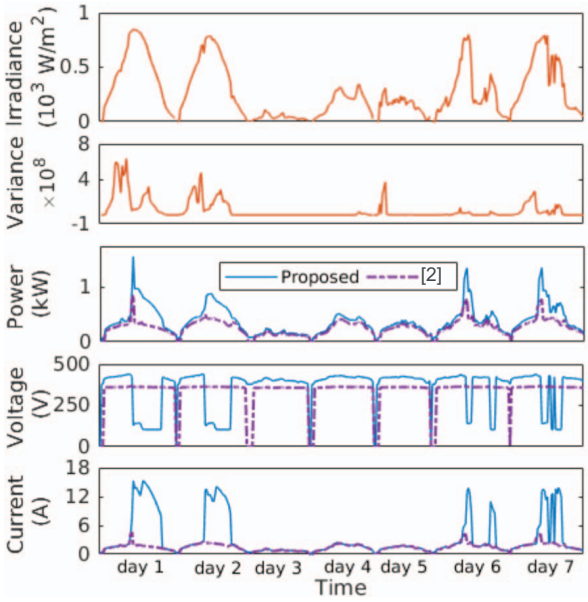

Figure 10. Snapshot of the simulation of the PV installation in Figure 8 when using the proposed model (solid lines) versus the model in [2] (dashed line).

4) Simulation results: To evaluate the features of the proposed diode-aware cell-based model, we compare its estimation w.r.t. another equation-based model, proposed in [2]. This model is empirical, as it is built from datasheet information. However, it targets the context of smart buildings, and thus reproduces the behavior of a PV module, with no detail on the inner organization of the module itself (e.g., number of diodes, behavior of each cell).

We simulated the behavior of the two models on a year-long trace of irradiance and temperature, and a snapshot corresponding to one week of simulated time is reported in Figure 10. The top of the Figure shows the evolution of irradiance over 7 days, plus its variance over the roof (the higher the variance, the more heterogeneous the distribution of G). The last three plots compare the power production estimated by the two models, where solid lines are the proposed model and dashed lines are for the model in [2].

Overall, the proposed model estimates +37.52% power production, i.e., 2.77MWh versus 2.01MWh. Figure 10 clarifies what generates such a huge difference. On days with high irradiance (e.g., days 1 and 2), the proposed model can benefit from the presence of diodes to sacrifice voltage and produce higher current. This is evident by considering the trace of voltage over time: the model in [2] has an almost constant voltage (unless when G is 0), while the voltage of the proposed model is subject to fluctuations. In correspondence to the periods with lower voltage, the current of the proposed model has peaks w.r.t. the model in [2], as an effect of the activation of bypass diodes. Vice versa, both models generate very similar traces on days with low variance (e.g., days 3-5).

This huge difference between the models is generated only by

the presence of diodes, given the similar construction process. The high improvement in terms of overall power production proves thus the importance of reproducing the presence of bypass diodes to gain an accurate figure of the behavior of the overall PV installation.

B. Comparison with power traces

In the second experiment, we compare the performance of the two models on traces extracted from a real PV installation. The roof of interest is an industrial roof with 4 parallel strings, each made of 10 modules in series. The measurements are extracted right before the inverter. The PV modules are Mitsubishi PV-MF165EB3 modules, with rated power 165W and made of 50 cells connected in series. We simulate one year of the PV installation with the model in [2], by assuming that each PV module is equipped with one dedicated bypass diode, and with the model proposed in this work, that reproduces the presence of 2 bypass diodes, each controlling 25 cells.

Figure 11 shows the evolution of irradiance over 7 days, its variance over the roof, plus the power production measured (black line) and estimated both with the model in [2] (solid line) and the currently proposed model (dashed line). The Figure highlights that both models approximate well the environmental traces: the error on the overall yearly power production is less then 2% for both models. However, the model proposed in this work achieves better accuracy: error on the yearly estimation is 0.29%, as opposed to an error of 1.21% of the model in [2]. This overall behavior is confirmed by two indicators that measure dispersion (the lower the value, the better [19]): the Root Mean Square Difference (RMSD, 20.29% versus 41.59%) and the coefficient of determination R^2 (i.e., the proportion between the variance and the predicted variable, 0.856 versus 0.866). Note that the accuracy improvement is achieved despite of a low variance of irradiance on the roof, as the building is quite isolated and the PV installation has been designed carefully to reduce partial shading to the minimum. Nonetheless, introducing sensitivity w.r.t. the presence of diodes allows to achieve a more accurate estimation, even if the model has been built solely with information derived from datasheets.

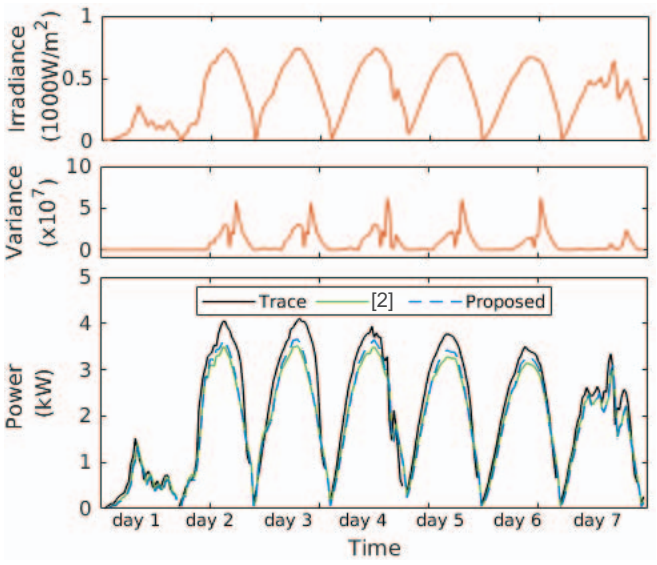

Figure 11. Snapshot of the simulation of a PV installation based on real measurements, by comparing traces (black line), the model proposed in [2] (dashed line), and the proposed model (solid line).

V. Conclusions

This paper proposed a model for PV modules that is aware of the presence of inner diodes. The model is built solely from information extracted from datasheets, thus being applicable to any PV module and not requiring extraction of electrical parameters or measurements. Our simulation results show that modeling the presence of diodes allows to achieve higher fidelity w.r.t. the behavior of PV installations under partial shading, thus achieving a more informed design.

References

[1] A. Dolara, S. Leva, and G. Manzolini, "Comparison of different physical models for PV power output prediction," vol. 119, 2015, pp. 83 – 99.

[2] S. Vinco, L. Bottaccioli, E. Patti, A. Acquaviva, and M. Poncino, "A compact PV panel model for cyber-physical systems in smart cities," in *Proc. of IEEE ISCAS*, 2018, pp. 1–5.

[3] A. Chatterjee, A. Keyhani, and D. Kapoor, "Identification of photovoltaic source models," *IEEE Transactions on Energy Conversion*, vol. 26, no. 3, pp. 883–889, Sep. 2011.

[4] M. Zagrouba, A. Sellami, M. Bouacha, and M. Ksouri, "Identification of PV solar cells and modules parameters using the genetic algorithms: Application to maximum power extraction," *Solar Energy*, vol. 84, no. 5, pp. 860 – 866, 2010.

[5] D. Sera, R. Teodorescu, and P. Rodriguez, "PV panel model based on datasheet values," in *Proc. of IEEE ISIE*, 2007, pp. 2392–2396.

[6] M. G. Villalva, J. R. Gazoli, and E. R. Filho, "Comprehensive approach to modeling and simulation of photovoltaic arrays," *IEEE Transactions on Power Electronics*, vol. 24, no. 5, pp. 1198–1208, 2009.

[7] S. Vinco, Y. Chen, E. Macii, and M. Poncino, "A unified model of power sources for the simulation of electrical energy systems," in *Proc. of ACM/IEEE GLSVLSI*, 2016, pp. 281–286.

[8] L. Benini, G. D. Micheli, E. Macii, M. Poncino, and R. Scarsi, "Symbolic synthesis of clock-gating logic for power optimization of control-oriented synchronous networks," in *Proc. of IEEE EDTC*, 1997.

[9] K. Ishaque, Z. Salam, H. Taheri, and Syafaruddin, "Modeling and simulation of photovoltaic (PV) system during partial shading based on a two-diode model," *Simulation Modelling Practice and Theory*, vol. 19, no. 7, pp. 1613 – 1626, 2011.

[10] A. Kajihara and A. T. Harakawa, "Model of photovoltaic cell circuits under partial shading," in *Proc. of IEEE ICIT*, 2005, pp. 866–870.

[11] M. G. Villalva, J. R. Gazoli, and E. R. Filho, "Comprehensive approach to modeling and simulation of photovoltaic arrays," *IEEE Transactions on Power Electronics*, vol. 24, no. 5, pp. 1198–1208, 2009.

[12] J. Kamala and A. Tamilarasi, "Characterization of PV cells with varying weather parameters to achieve maximum power," in *Proc. of IEEE ICECS*, 2015, pp. 21–26.

[13] A. Smets, K. Jager, O. Isabella, R. van Swaaij, and M. Zeman, *Solar Energy: The physics and engineering of photovoltaic conversion, technologies and systems*. UIT Cambridge, 2016.

[14] D. J. Pagliari, S. Vinco, E. Macii, and M. Poncino, "Irradiance-driven partial reconfiguration of PV panels," in *Proc. of DATE*, 2019, pp. 884–889.

[15] PEIMAR, "Residential line SG280P," http://www.peimar.com/datasheet/Peimar_IT_SG280P.pdf, 2010.

[16] F. Brihmat and S. Mekhtoub, "PV cell temperature/PV power output relationships Homer methodology calculation," in *IJSET*, vol. 1, 2014.

[17] L. Bottaccioli, E. Patti, E. Macii, and A. Acquaviva, "GIS-based software infrastructure to model PV generation in fine-grained spatio-temporal domain," *IEEE Systems Journal*, vol. 12, no. 3, pp. 2832–2841, 2018.

[18] S. Vinco, L. Bottaccioli, E. Patti, A. Acquaviva, E. Macii, and M. Poncino, "GIS-based optimal photovoltaic panel floorplanning for residential installations," in *Proc. of DATE*, 2018, pp. 437–442.

[19] F. Spertino and F. Corona, "Monitoring and checking of performance in photovoltaic plants: A tool for design, installation and maintenance of grid-connected systems," *Renewable Energy*, vol. 60, pp. 722 – 732, 2013.